APPLICATION OF AN ARM-BASED FDM SYSTEM FOR SANDWICH PANEL FABRICATION

D. Pollard[1], G. Herrmann[2], C. Ward[3], and J. Etches[3]

[1]Bristol Robotics Laboratory, University of the West of England, T Block, Frenchay Campus Coldharbour Lane, Bristol, BS16 1QY, United Kingdom
Email: d.pollard@bristol.ac.uk
[2]Department of Mechanical Engineering, University of Bristol, Queens Building, University Walk, Bristol, BS8 1TR, United Kingdom
[3]Bristol Composites Institute (ACCIS), University of Bristol, Queens Building, University Walk, Bristol, BS8 1TR, United Kingdom

Keywords: Robotic Printing, Core Manufacture, Additive Manufacture, FDM, FFF

Abstract
Fused Deposition Modelling (FDM), a form of additive manufacture, is typically constrained to 2.5D, vertically stacked layers; curved layers have been shown to possess improved mechanical properties and surface finish but require complex toolpath generation. This paper demonstrates methods of generating thin-walled FDM components with curved layers suited for use within aerospace composite sandwich panels; secondary structures containing high complexity and low production volumes ripe for manufacture using additive techniques.

An industrial robot arm and a PC-based open-source controller allowed for significantly higher degrees of toolpath complexity for FDM than realised using conventional systems. Three use cases are presented to describe the manufacture of FDM components, with the first demonstrating deposition on a rotating cylinder, allowing for customised stiffening and reinforcement. The second shows a curved surface defined by an STL file, with the nozzle orientated to remain perpendicular to the surface, and finally the manufacture of a shaped aerofoil cores with curved layers conforming to the outer surfaces. The application developed over the course of this work shows the high levels of manufacturing flexibility achievable with arm-based FDM, and its potential use within the aerospace industry where optimised and complex components are manufactured in low volumes.

1. Introduction

Additive Manufacture (AM) is a process which allows the manufacture of components directly from digital CAD data through the deposition of successive layers of material, enabling the economic productions of complex geometries in low production volumes [1, 2]. Fused Deposition Modelling (FDM) is an AM process where molten polymer is extruded through a moving nozzle, typically mounted to a gantry-style 3-DOF system. Within the aerospace industry, AM technologies are well suited to the required complexity and production volumes realised, with materials such as Ultem 9085 certified for use within aerospace cabin components [3].

Sandwich panels, commonly used as secondary structures in the aerospace industry, are comprised of a core material placed between two high modulus face sheets, providing an excellent stiffness to weight ratio in complex geometries [4, 5]. Traditional manufacture involved cores being comprised of multiple sections of Nomex honeycomb spliced together to meet geometric and strength requirements; FDM has been shown to be suited to the manufacture of such complex cores, with previous work demonstrating

the application of thicker walls for local reinforcement on a double curvature panel [6], the achievement of higher strengths than Nomex [7], and the capability of manufacturing cores with curved layers [8].

The deposition of curved layers provides significant advantages over the traditional, vertically stacked, "2.5D" manufacture. Strong anisotropy exists in FDM components due to the inter-layer bonding [9], however Singamneni et al. have shown that a bridge-shaped structure printed with curved layers can possess significantly higher strength under a three-point bend test than that manufactured using traditional FDM [10]. A constraining factor is the limited software available for curved layer slicing, with most code written specifically for a given application; a review of curved layer slicing approaches was undertaken by Zhao et al. [11].

The traditional gantry-style printers are unsuited for curved layer manufacture due to the low *z* axis speed limiting the available curvature [8, 12]. Delta robots are capable of manufacturing layers with higher curvature [8], but the maximum curvature is constrained by the constant orientation of the print head risking collision with the component. To reliably manufacture curved layers over a variety of shapes, higher degree of freedom (DOF) systems must be used, with Stewart Platforms used by Song et al. [13] to demonstrate the capability of scanning and printing directly onto a curved surface, and Dröder et al. [14] presenting the concept of "Additive Finalisation", where a mass produced base component has finishing features deposited by FDM.

Robotic arms have a significantly larger workspace than other structural layouts, and the capability to orientate the FDM nozzle in up to 6-DOF [12]. A project at MIT demonstrated compound fabrication, with high speed deposition of a foam structure followed by subtractive machining to achieve a higher dimensional accuracy [15]. Several academic institutions are currently investigating the use of robotic arms for additive manufacture, such as Brooks et al. [16] from Massey University, NZ, demonstrating the use of a fixed extruder for deposition on a hemispherical mandrel held by a 6-DOF robot arm. More conventional layouts with a fixed bed and movable extruder include Beihang University, China [11], Virginia Tech, USA [17], and Florida University, USA [18]. Within industry, Stratasys demonstrated the "Infinity Build" concept, showcasing tool changing capabilities and additive finalisation onto curved surfaces targeted at the automotive and aerospace industries [19], and arm-based AM has been implemented by a number of construction companies for architectural projects [20].

This paper begins with an introduction to the robotic FDM system developed at the University of Bristol. Descriptions of the process to generate print paths for the localisation and manufacture of a structure on a rotating cylinder, and deposition onto a curved substrate are presented, and followed by a demonstration of manufacture of an aerofoil-shaped structure with curved layers. Finally, the conclusions are presented with details of future work.

2. Robotic arm-based FDM system

The robotic cell at the University of Bristol is comprised of a 6-DOF ABB IRB 140 arm with a 2-DOF IRBP A250 positioner, powered and controlled through an IRC5 controller; the robot cell is shown in Figure 1. An FDM nozzle was attached as an end effector, comprised of a BondTech extruder with an E3D v6 hotend, with temperature and extrusion speed regulation provided through an Arduino Mega with a RAMPS 1.4 breakout board. A 0.6 mm nozzle provided a balance between print quality and maximum print speed.

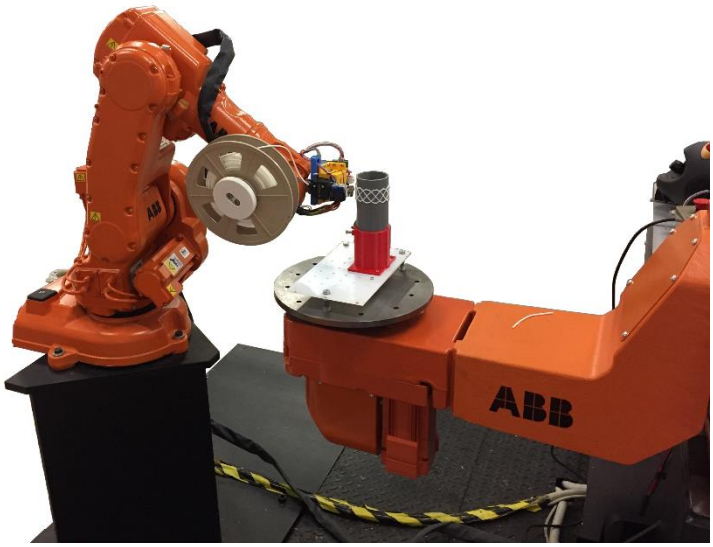

Figure 1: ABB Robot Cell at the University of Bristol consisting of an ABB IRB 140 arm and IRBP A250 positioner

RAPID is the native language implemented on the IRC5 controller for robot positioning, but due to the complex toolpaths required for FDM objects, it is desirable to control the robot directly from a PC; Brooks et al. estimated the full print would consist of 180,000 lines of RAPID code [16]. PC control was achieved over an Ethernet connection through the adaption of the open source Open-ABB software package [21], with an extra implementation of an increased buffer complexity to transmit, store, and execute movements, with the adapted code available at [22]. Digital signals from the IRC5 controller supplied the extruder with the on/off demand and the required extrusion speed; a more detailed description is provided in [12].

To generate a toolpath to manufacture an FDM component, the transformation from the robot base frame to the work object coordinate system, and from the tool centre point (TCP) to the nozzle tip was first defined; in a majority of cases these are direct translations. A series of poses are then supplied with a Cartesian position and a quaternion describing the transformation from the work object coordinate system to the tool coordinate system; an additional option allows for positioner movement, as used in Section 3. This buffer is then executed with "fine" movements at the beginning and end of the executed poses to ensure the digital output to the extruder is synchronised with the motion. All toolpath generation and control software on the PC was implemented using Python 2.7.

3. Cylindrical core manufacture

3.1 Localisation of cylinder in relation to robot base frame

As there were no sensors fitted to the robot arm to track the location of the cylinder, the kinematics between the base coordinate frame of the robot ($c_0=xyz_0$) and the position on the cylinder surface during a rotational movement must be first identified. This was comprised of the transformation from c_0 to the centre of rotation ($c_1=xyz_1$), the rotation about the z axis of c_1 to a rotated coordinate frame ($c_2=xyz_2$), and the location of the cylinder within c_2 (x_{cyl}, y_{cyl}); this is depicted in Figure 2, with the associated kinematics in *(1a)*. As all z axes were aligned, the problem was reduced to 2 dimensions, with the z transformation from c_0 to c_1 identified through measurement.

Four 2D linear translation parameters were required for the kinematic equation *(1a)*; from c_0 to c_1 (x_1, y_1), and the cylinder location (x_{cyl}, y_{cyl}) within c_2, This provided an estimate of the cylinder position (x_{est}, y_{est}) in the robot base coordinate frame for a given rotation θ. For parameter identification, the nozzle was positioned on the cylinders circumference at n different rotations, providing three measured

coordinates ($x_{n,\,meas}$, $y_{n,\,meas}$, $\theta_{n,\,meas}$). An optimisation routine minimised the cost function of *(1b)* through variation of the linear translation parameters in *(1a)*, comparing the difference between estimated and measured coordinates for each rotation angle $\theta_{n,\,meas}$.

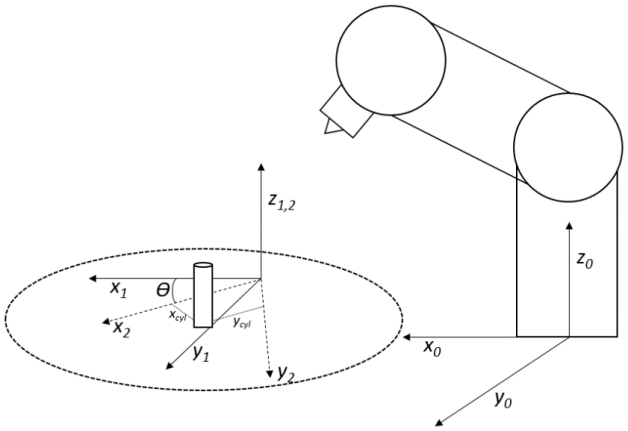

Figure 2: Transformation from robot base frame to the rotated coordinate system on the positioner.

$$\begin{bmatrix} x_{n,\ est} \\ y_{n,\ est} \end{bmatrix}_{C_0} = \begin{bmatrix} x_1 \\ y_1 \end{bmatrix}_{c_0} + \begin{bmatrix} \cos\theta_n & -\sin\theta_n \\ \sin\theta_n & \cos\theta_n \end{bmatrix} \begin{bmatrix} x_{cyl} \\ y_{cyl} \end{bmatrix}_{c_2} - r_{cyl} \begin{bmatrix} \cos\theta_n \\ \sin\theta_n \end{bmatrix} \tag{1a}$$

$$cost = \frac{1}{2n} \sum_{n} \left| x_{n,\ est} - x_{n,\ meas} \right| + \left| y_{n,\ est} - y_{n,\ meas} \right| \tag{1b}$$

3.2 Generation of cylindrical toolpath

A planar 2D toolpath was generated, consisting of points ($x_{i,\,path}$, $y_{i,\,path}$), to be "wrapped" around the cylinder surface. x_{path} was mapped to the cylinder rotation angle θ based on the arc length around the circumference, as shown in *(2a)*, and y_{path} was mapped directly to the nozzle *z* height, as shown in *(2b)*.

The cylinder offset from the centre of rotation caused a displacement in the *xy* plane of c_1 upon rotation; *(2c)* provided the required offset for the nozzle in the coordinate frame c_1 to track the cylinder surface. The full coordinates required for the robot to print on the cylindrical surface were the rotation of the cylinder on the positioner θ_i, the nozzle position (x_i, y_i, z_i) in c_1, and the nozzle orientation, held constant at normal to the cylinder surface, depicted in Figure 3.

$$\theta_i = \frac{x_{\,i,\ path}}{r_{cyl}} \tag{2a}$$

$$z_i = y_{i,\ path} \tag{2b}$$

$$\begin{bmatrix} x_i \\ y_i \end{bmatrix}_{c_1} = \begin{bmatrix} \cos\theta_i & -\sin\theta_i \\ \sin\theta_i & \cos\theta_i \end{bmatrix} \begin{bmatrix} x_{cyl} \\ y_{cyl} \end{bmatrix}_{c_2} \tag{2c}$$

To demonstrate this process, the 2D toolpath was extracted from the Scalable Vector Graphics (SVG) file of the University of Bristol logo, and a corresponding print path calculated. The result from a visualisation of the toolpath and the actual path is shown in Figure 3.

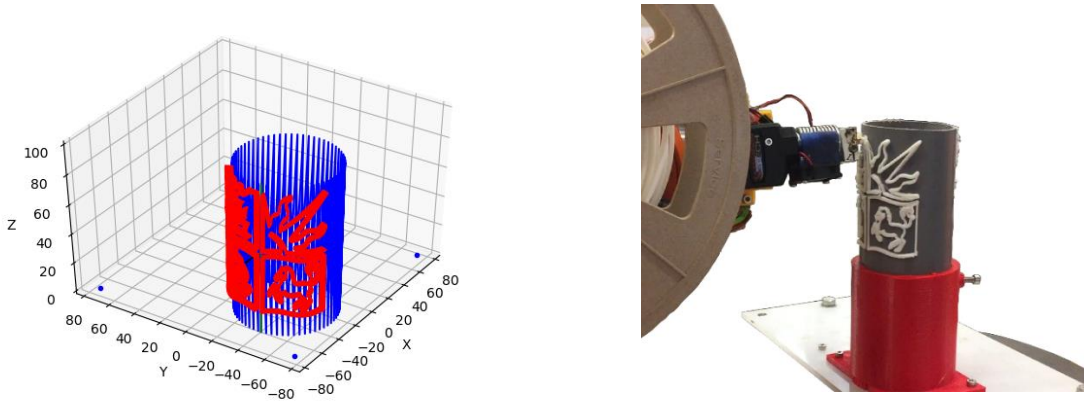

Figure 3: Visualisation *(left)* and realisation *(right)* of a 2D print path generated from an SVG file mapped onto a cylinder.

4. Curved core generation

4.1. Printing onto curved surface

To generate the toolpath for a curved surface, an STL input file was used to describe the substrate surface; this is a standard CAD export format typically used within FDM slicing programs, which describes a 3D model as a series of tessellated triangles, with each facet containing three coordinates and a surface normal away from its surface. An additional benefit was the ability to directly manufacture with a traditional FDM printer prior to testing.

The STL file was imported using the Python STL library, and rotated, translated and trimmed to contain facets from the top surface. A projection of the 2D toolpath provided the required *z* coordinate for each point, and the surface normal for each point was obtained from the surface normal of the enclosing facet. For deposition of successive layers, the point was offset in the direction of this normal, described below, or in the *z* direction, demonstrated in Section 4.2. Collisions with the prebuilt surface during travel moves were avoided by execution of a circular path between two print lines. An example deposition using this process is shown in Figure 4, where the logo print path used in Section 3 was deposited directly onto a hemispherical shape.

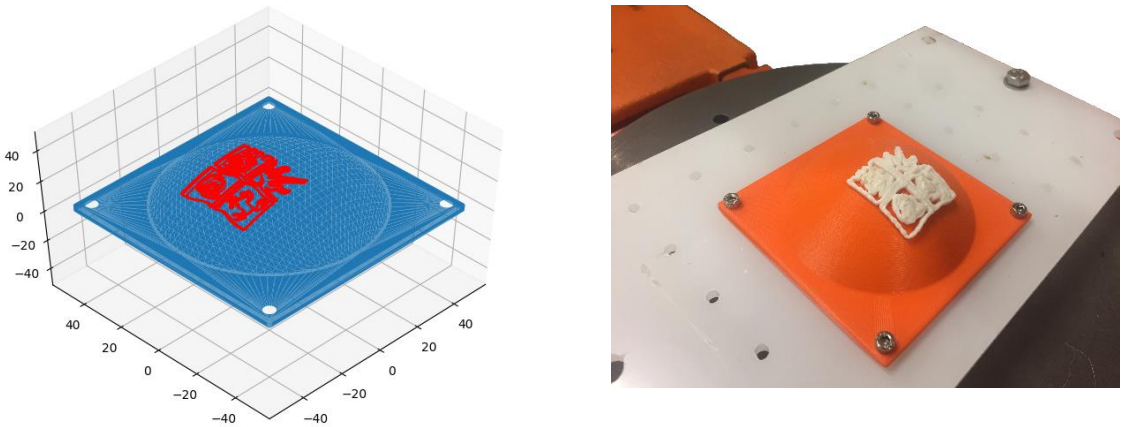

Figure 4: Visualisation *(left)* and realisation *(right)* for deposition of a honeycomb structure onto a hemispherical surface with the print direction following the surface normal.

The quaternion required to maintain the correct nozzle orientation, q_{nozzle}, relative to the work object coordinate system c_1, was generated based on the surface normal, $\boldsymbol{n} = (n_x, n_y, n_z)$ and its angle to the x and y axis vectors, $\boldsymbol{x} = (1, 0, 0)$ and $\boldsymbol{y} = (0, 1, 0)$ respectively. The calculation is shown in *(3)*. An addition of π to the angle to the x axis provides the 180° rotation to orient the z axis of the TCP to the opposing direction to n_z.

$$q_x = \left[\cos\left(\frac{\theta_x}{2}\right), 0, \sin\left(\frac{\theta_x}{2}\right), 0\right] \text{ where } \theta_x = \sin^{-1}\frac{(n_x, 0, n_z)\,.\,\boldsymbol{x}}{\|(n_x, 0, n_z)\|} + \pi \tag{3a}$$

$$q_y = \left[\cos\left(\frac{\theta_y}{2}\right), \sin\left(\frac{\theta_y}{2}\right), 0\,, 0\right] \text{ where } \theta_y = \sin^{-1}\frac{(0, n_y, n_z)\,.\,\boldsymbol{y}}{\|(0, n_y, n_z)\|} \tag{3b}$$

$$q_{nozzle} = q_x \times q_y \tag{3c}$$

4.2. Manufacture of curved layer component

Two aerofoil cores were manufactured to demonstrate applicability to the aerospace industry; a straight, untwisted aerofoil and a tapered aerofoil including twist. The bottom surface of each specimen was again described by an STL file, and a 2D hexagonal toolpath generated to cover the aerofoil surface, with the conforming layer generated as in Section 4.1. Successive layers of deposition were generated through application of an offset along the z axis, with points higher than the centre line removed; the resulting half was then reflected to produce the upper half, curved in the opposing direction; this is shown by the top and bottom toolpaths generated as shown in Figure 5, depicting the straight and untampered aerofoil.

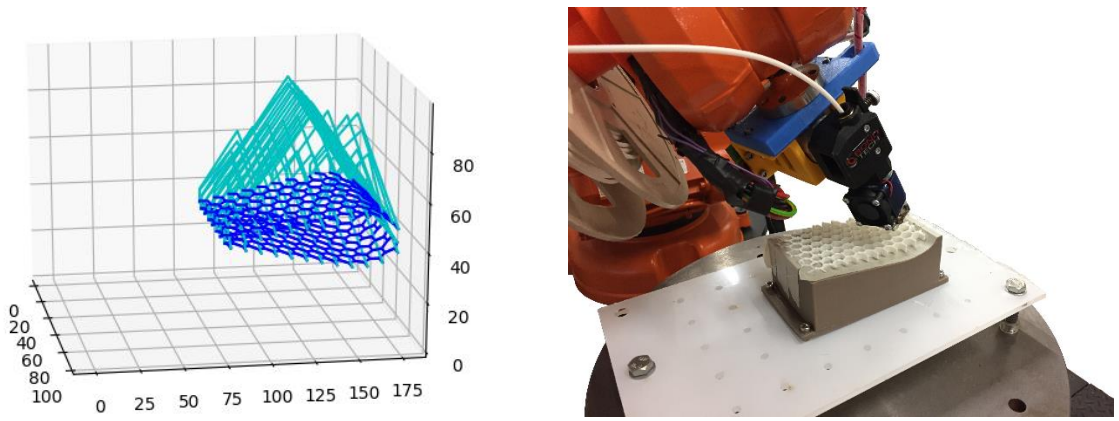

Figure 5: Visualisation *(left)* of the top and bottom layers path travel, and realisation *(right)* of an untapered aerofoil shape. The lighter coloured lines depict circular travel movements to avoid collision with the existing structure.

Further expansion allowed for a variable z height along the path layer, calculated from the vertical intersection with a second STL file denoting the top surface. This allowed the manufacture of a curved and tapered aerofoil shape, showing the high levels of complexity achievable with a robotic arm. This is depicted in Figure 6, where a twisted and curved aerofoil was printed; two STL files were created to define the shape with the first defining the centre plane, and the second using a "loft" feature to create the aerofoil shape along this plane.

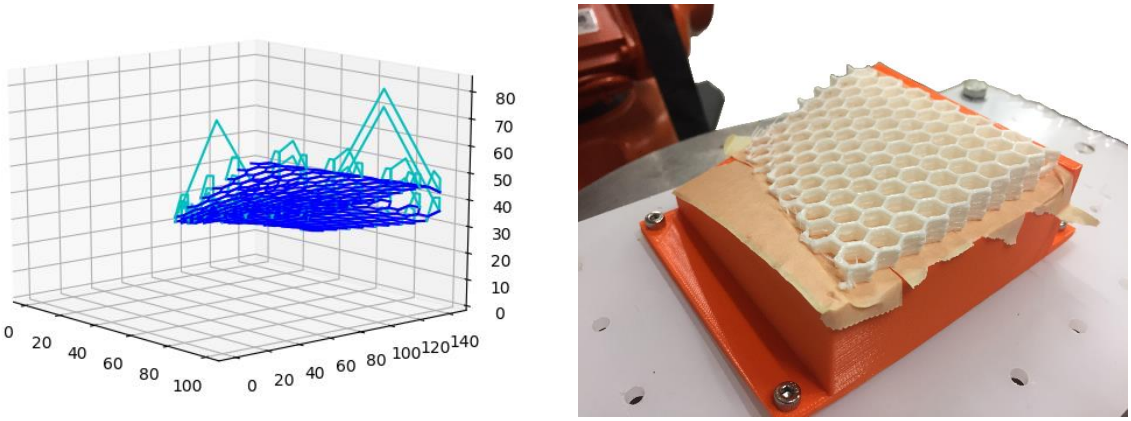

Figure 6: Visualisation *(left)* and realisation *(right)* of a complex aerofoil shape manufactured with curved layer FDM.

5. Conclusions

The use of robotic arm-based Fused Deposition Modelling (FDM) provided the low-cost and high complexity achievable through conventionally manufactured FDM components with the added capability of the in-situ manufacture of curved layers, requiring a greater degree of complexity for toolpath generation. This work has introduced methods to map a SVG graphics file to robot coordinates for printing directly onto a cylindrical surface located in the robots workspace, and to map a 2D toolpath onto a curved surface defined by an STL file. Finally, aerofoil-shaped cores were produced demonstrating the capability to produce print exterior layers anticipated to possess improved mechanical properties.

The increased ease of toolpath generation for robotic arms described in this work will aid adoption of complex FDM within the aerospace industry. The controller has additional uses due to its flexibility for toolpath generation which remain to be explored, such as for tow-steering in AFP, and the ability to process complex sensor data on the PC and modify toolpaths to enable cobotic layup and manufacture.

Further work will investigate the use of a 3D scanner to aid the initial localisation procedure and to generate the initial STL file for substrate printing. Additional work will involve the assessment of different methods of transitioning between layer curvatures taking inspiration from ply-drop literature.

6. Acknowledgements

This work was supported by the EPSRC Centre for Doctoral Training in Future Autonomous Robotic Systems (FARSCOPE) at the Bristol Robotics Laboratory (grant EP/L015293/1).

The data necessary to support the conclusions are included within this paper. The code is available under the MIT license and a video showing the robot operation are available at the following URLs:

https://github.com/davepollard/CurvedLayer_FDM

Curved Layer FDM with a robotic arm: https://www.youtube.com/watch?v=v36t1wzLFEM

7. References

[1] ISO Standard, "ISO/ASTM 52900:2015 Additive manufacturing - General principles - terminology," 2015.

[2] T. Wohlers, "Wohler's report 2013", 2013.

[3] Stratasys, "ULTEM 9085 Data Sheet," 2017.

[4] D. Zenkert, An introduction to sandwich construction, Engineering materials advisory services, 1997.

[5] C. Ward, K. Hazra and K. Potter, "Development of the manufacture of complex composite panels," *International Journal of Materials and Product Technology,* vol. 42, pp. 131-155, 2011.

[6] F. Riss, J. Schilp and G. Reinhart, "Load-dependent Optimization of Honeycombs for Sandwich Components - New Possibilities by Using Additive Layer Manufacturing," *Physics Procedia,* vol. 56, pp. 327-335, 2014.

[7] D. Pollard, C. Ward, G. Herrmann and J. Etches, "The manufacture of honeycomb cores using Fused Deposition Modeling," *Advanced Manufacturing: Polymer & Composites Science,* vol. 3, pp. 21-31, 2017.

[8] R. J. A. Allen and R. S. Trask, "An experimental demonstration of effective Curved Layer Fused Filament Fabrication utilising a parallel deposition robot," *Additive Manufacturing,* vol. 8, pp. 78-87, 2015.

[9] J. F. Rodríguez, J. P. Thomas and J. E. Renaud, "Mechanical behavior of acrylonitrile butadiene styrene fused deposition materials modeling," *Rapid Prototyping Journal,* vol. 9, pp. 219-230, 2003.

[10] S. Singamneni, A. Roychoudhury, O. Diegel and B. Huang, "Modeling and evaluation of curved layer fused deposition," *Journal of Materials Processing Technology,* vol. 212, pp. 27-35, 2012.

[11] G. Zhao, G. Ma, J. Feng and W. Xiao, "Nonplanar slicing and path generation methods for robotic additive manufacturing," *The International Journal of Advanced Manufacturing Technology,* pp. 1-11, 2018.

[12] D. Pollard, G. Herrmann, C. Ward and J. Etches, "A Comparison of FDM Structural Layouts and Implementation of an Open-Source Arm-Based System," *International Conference on Mechanical, Manufacturing, Modeling and Mechatronics (IC4M),* vol. 167, 2018.

[13] X. Song, Y. Pan and Y. Chen, "Development of a Low-Cost Parallel Kinematic Machine for Multidirectional Additive Manufacturing," *Journal of Manufacturing Science and Engineering,* vol. 137, p. 021005, 2015.

[14] K. Dröder, J. K. Heyn, R. Gerbers, B. Wonnenberg and F. Dietrich, "Partial Additive Manufacturing: Experiments and Prospects with Regard to Large Series Production," *Procedia CIRP,* vol. 55, pp. 122-127, 2016.

[15] S. Keating and N. Oxman, "Compound fabrication: A multi-functional robotic platform for digital design and fabrication," *Robotics and Computer-Integrated Manufacturing ,* vol. 29, pp. 439-448, 2013.

[16] B. J. Brooks, K. M. Arif, S. Dirven and J. Potgieter, "Robot-assisted 3D printing of biopolymer thin shells," *The International Journal of Advanced Manufacturing Technology,* pp. 1-12, 2016.

[17] J. R. Kubalak, et al., "Design and Realization of a 6 Degree of Freedom Robotic Extrusion Platform," in *Proceedings of the Solid Freeform Fabrication Symposium*, 2016.

[18] I. B. Ishak, J. Fisher and P. Larochelle, "Robot Arm Platform for Additive Manufacturing Using Multi-Plane Toolpaths," in *ASME 2016 International Design Engineering Technical Conferences and Computers and Information in Engineering Conference*, 2016.

[19] Stratasys Ltd., "Stratasys demonstrates next generation 3D printing technology designed to break barriers in part performance and production efficienct for aerospace and automotive manufacturing," *Press Release,* 24/8/2016.

[20] L. Williams, "Cities Rising: Using 3D Printing to Build Houses," *Institute of Mechinical Engineers,* 2017.

[21] M. Dawson-Haggerty, "Open-ABB," 2016. [Online]. Available: https://github.com/robotics/open_abb.

[22] D. Pollard, "OpenABB-FDM," 2018. [Online]. Available: https://github.com/bristolroboticslab/OpenABB-FDM.